Journal of
Materials Chemistry A

PAPER

Cite this: *J. Mater. Chem. A*, 2017, **5**, 10424

Simple structured polyetheramines, Jeffamines, as efficient cathode interfacial layers for organic photovoltaics providing power conversion efficiencies up to 9.1%†

Bing-Huang Jiang, Ya-Juan Peng and Chih-Ping Chen *

Received 5th April 2017
Accepted 25th April 2017

DOI: 10.1039/c7ta02954c

rsc.li/materials-a

In this study, we have found that interfacial layers (IFLs) based on Jeffamines (industrial polyetheramine derivatives) can improve the performance of organic photovoltaics (OPVs). We evaluated four different Jeffamines (average molecular weight: 2000 g mol^{-1})—M2005, M2070, D2000, and ED2003—having either a monoamine or diamine structure and various ratios of propylene oxide (PO) and ethylene oxide (EO) for their suitability as IF materials for OPV applications. The presence of the Jeffamine altered the work function of ZnO and improved the electron transport, thereby causing the ZnO layers to function more efficiently as electron-selective electrodes. The power conversion efficiencies (PCEs) of inverted devices having the layered configuration glass/indium tin oxide (ITO)/ZnO (with or without the Jeffamine)/PTB7:PC$_{71}$BM/MoO$_3$/Ag increased from 8.1 ± 0.11 to 8.6 ± 0.37% when containing the Jeffamine-D2000 under illumination with AM 1.5G solar light (1000 W m^{-2}), the result of a significantly increased fill factor (FF). The greatest OPV performance was that of the device incorporating Jeffamine-D2000—a PCE of 9.1% and a remarkable FF of 74.2%.

Introduction

Great efforts have been exerted in the development of roll-to-roll, low energy consumption, cost-effective organic photovoltaics (OPVs) as promising alternatives to traditional PVs for certain applications.[1–5] Advances in materials development and device engineering have led to the power conversion efficiencies (PCEs) of bulk-heterojunction (BHJ) OPVs reaching 12%.[6–14] Interfacial (IF) layers play a significant and unique role in the enhanced performance of OPVs.[15–18] Many IF materials have been tested successfully, including self-assembled layers,[19] polyelectrolytes,[20–22] non-conjugated organic materials[7] [*e.g.*, polyethylenimines (PEIs) and their ethoxylated derivatives (PEIEs)],[23,24] and organic and inorganic hybrid materials.[25–27] Several mechanisms have been proposed to explain how IFLs improve the performance of OPVs; for example, by suppressing carrier recombination,[28] improving charge extraction to minimize series resistance,[29] altering the work function (built-in dipole) to facilitate efficient energy level pinning for high-performance carrier extraction,[30,31] smoothening the surface of ZnO,[32] and changing the BHJ morphology of the active layers[33] for efficient charge transfer and transportation (well-defined nanoscale phase segregation or a gradient distribution of the donor/acceptor morphology for enhanced carrier transport).[24] The most studied cathode modifying layers, PEIs and PEIEs, form efficient interface dipoles on the cathode and, hence, change the work function (WF) of the electron transporting layer (ETL) or cathode, thereby improving carrier extraction.[34,35]

In this study, we evaluated four Jeffamines [average molecular weight (MW): 2000 g mol^{-1}]—M2005, M2070, D2000 and ED2003, having monoamine or diamine structures and various ratios of propylene oxide (PO) and ethylene oxide (EO)—for their suitability for use as efficient cathode-modifying layers for OPV applications (Fig. 1). Jeffamines are polyetheramines that feature primary amino groups end-capping a polyether backbone. Because of the wide range of possible MWs, amine functionality, and types of repeating units, Jeffamines can provide flexibility for specific applications.[36] More importantly, these materials are very cheap and they are used industrially as additives for polyurethane

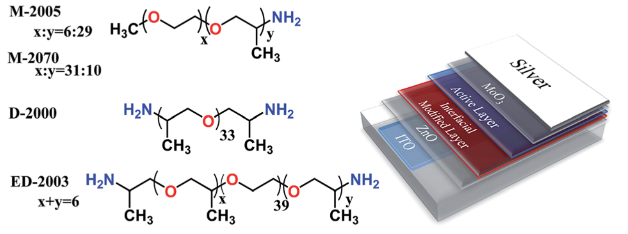

Fig. 1 Schematic representation of the OPV device; chemical structures of the Jeffamines.

Department of Materials Engineering, Ming Chi University of Technology, 84 Gunjuan Road, Taishan, New Taipei City, 24301, Taiwan. E-mail: cpchen@mail.mcut.edu.tw

† Electronic supplementary information (ESI) available. See DOI: 10.1039/c7ta02954c

elastomers and foams. Here, we examined Jeffamines as ETL–IF layers for inverted OPVs and evaluated how their surface properties (surface energy and morphology) and WFs changed the morphologies and optoelectronic properties of the BHJ layers and the performance of their related devices. We studied the effects of these IFLs on the space-charge limited current (SCLC) electron mobilities, the active layer morphologies, the monochromatic incident photon-to-electron conversion efficiencies (IPCEs), and the PCEs of devices incorporating an active layer comprising a polybenzodithiophene derivative (PTB7) and a fullerene derivative ($PC_{71}BM$). We observed an enhancement in performance from 8.1 ± 0.11 to 8.6 ± 0.37% when the device contained the Jeffamine D2000. The highest PCE (9.1%) was accompanied by a remarkable fill factor (FF) of 74.2%. A key feature resulting in the high PCEs was the improved electron extraction [electron mobility increased from 1.24×10^{-8} ($\pm 1.86 \times 10^{-9}$) to 3.06×10^{-8} ($\pm 1.07 \times 10^{-9}$) $m^2\ V^{-1}\ s^{-1}$], due to changes in the morphology and in the WFs of ZnO. As noted by Su and coworkers, only a few OPV devices have been reported having FFs greater than 74%.[28] Varying the intrinsic properties of the donor or acceptor (high and balanced carrier mobility) and morphological control (over the blend film domain sizes, the π–π stacking distance and direction, the gradient distribution of the BHJ for selective carrier transport, and IF modification) can have significant effects leading to high FFs.[28] Our results suggest that judicious selection of materials in the IF layer can be used to optimize charge extraction, recombination, and extraction within OPV devices to ensure high performance and a high FF.[37,38]

Results and discussion

We prepared ZnO layers on a pre-patterned ITO substrate using a zinc acetate precursor solution in 2-methoxyethanol (2-ME). The ZnO films were annealed at 160 °C for 30 min in air prior to the deposition of the Jeffamine. Solutions of the Jeffamines were prepared by dissolving them in 2-ME at a concentration of 0.3 wt%. These solutions were deposited on top of the ZnO layers through spin-coating (5000 rpm) in air and then the ZnO samples were dried (100 °C, 10 min) in a glovebox. The surficial status of the substrate [characterized by the surface energy (γ_{total}), which is equal to the sum of dispersive ($\gamma_{dispersive}$) and polar (γ_{polar}) components] had significant effects on the morphology of the BHJ, the carrier transport, and the related OPV performance.[24,39,40] We performed contact angle measurements using distilled H_2O and diiodomethane (CH_2I_2, DIM) as probe liquids[39] to calculate the values of γ_{total} (from the Wu model)[40] of the ZnO surfaces and, thereby, examine the effects of the Jeffamines. Table 1 lists the values of the components $\gamma_{dispersive}$ and γ_{polar} and the values of γ_{total} of the films of ZnO prepared with and without the various Jeffamines. The values of γ_{total} of the as-cast films of ZnO, ZnO/M2005, ZnO/M2070, ZnO/D2000, and ZnO/ED2003 were 70.43, 67.10, 73.79, 76.46, and 75.82 mN m^{-1}, respectively. The value of γ_{total} of the ZnO film was almost identical to those reported in the literature.[40] The values of γ_{total} for the Jeffamine-modified ZnO films varied widely. For the monoamines M2005 and M2070, the different PO to EO ratios appeared to affect the surface energy. The high EO ratio of M2070 resulted in a low value of θ_{water} and higher value of γ_{polar}. The values of γ_{total} for the films embedding the diamine-based Jeffamines (D2000 and ED2003) were higher than those featuring the monoamine Jeffamines. Because the value of γ_{total} for a surface affects the deposition behavior of solvents and solutions, it also determines the quality of the film that formed. A high value of γ_{total} suggests more ready adhesion to contacting materials.[41] The surface properties of ZnO will affect its optoelectronic properties as well as the morphology of the active layer and its corresponding OPV performance.[40,42] The diamine Jeffamines (D2000 and ED2003) provided larger surface energies, potentially affecting the wetting properties of the solution of the active layer and, thereby, altering the morphology of the BHJ layer. Fig. S1† displays tapping-mode atomic force microscopy (AFM) images of the ZnO films. The root mean square (RMS) surface roughnesses of the ZnO film and those embedding M2005, M2070, D2000, and ED2003 were 2.4, 2.2, 2.6, 2.7, and 3.1 nm, respectively. Thus, the topographic images of the ZnO films suggested that the deposition of the Jeffamines onto the ZnO layers did not significantly alter their topographical morphologies.

We fabricated OPV devices having an inverted architecture with a layer structure: ITO glass/ZnO (with or without a Jeffamine)/$PTB7:PC_{71}BM/MoO_3$ (3 nm)/Ag (100 nm).[24,43] The ESI† provides details of their fabrication and the testing conditions. We denote the standard cell (without the IFLs) as the ZnO device, and the devices containing the various IFLs as the M2005, M2070, D2000, and ED2003 devices. Table 2 summarizes the average and best OPV performances of the devices. The average values and standard deviations in Table 2 were calculated from 10 cells. The standard ZnO device had a PCE of 8.1 ± 0.11% under AM 1.5G illumination (100 mW cm^{-2}), with a value of J_{sc} of 15.7 ± 0.33 mA cm^{-2}, a value of V_{oc} of 0.72 ± 0.01 V, and an FF of 71.6 ± 2.28%. This PCE is comparable with those of $PTB7/PC_{71}BM$ devices reported in the literature.[44,45] The PCEs of the devices embedding M2005, M2070, D2000, and ED2003 were 7.8 ± 0.18, 7.5 ± 0.29, 8.6 ± 0.37, and 8.0 ± 0.42, respectively. The highest PCE of 9.1% was observed with a value of J_{sc} of 16.8 mA

Table 1 Contact angle (θ) and surface energy data for the ZnO films

ETL	θ_{water} [°]	θ_{DIM} [°]	γ_{polar} [mN m^{-1}]	$\gamma_{dispersive}$ [mN m^{-1}]	γ_{total} [mN m^{-1}]
ZnO	35.99	36.54	28.72	41.71	70.43
M2005	40.87	39.83	26.87	40.42	67.10
M2070	29.45	34.74	31.30	42.49	73.79
D2000	17.20	39.97	36.28	40.17	76.46
ED2003	29.26	27.90	30.36	45.22	75.82

Table 2 *J–V* properties of the OPV devices

Devices	J_{sc} (mA cm^{-2})	V_{oc} (V)	FF (%)	PCE (%)	Best PCE (%)	R_{sh} (Ω cm^2)	R_s (Ω cm^2)
ZnO	15.7 ± 0.33	0.72 ± 0.01	71.6 ± 2.28	8.1 ± 0.11	8.2	1086 ± 314	2.0 ± 0.2
M2005	15.0 ± 0.21	0.73 ± 0.01	71.7 ± 1.22	7.8 ± 0.18	8.0	1438 ± 628	1.9 ± 0.1
M2070	14.6 ± 0.53	0.73 ± 0.01	71.2 ± 2.29	7.5 ± 0.29	7.9	975 ± 254	2.0 ± 0.1
D2000	15.9 ± 0.89	0.73 ± 0.01	74.6 ± 0.99	8.6 ± 0.37	9.1	2118 ± 672	1.5 ± 0.2
ED2003	15.4 ± 0.06	0.73 ± 0.01	71.4 ± 3.00	8.0 ± 0.42	8.3	1040 ± 632	2.0 ± 0.2

cm^{-2}, a value of V_{oc} of 0.73 V, and an FF of 74.2% (Fig. 2a, Table 2). Compared with the ZnO device, the PCE for the D2000 device had increased by 11%. We determined the series (R_s) and shunt (R_{sh}) resistances from the respective *J–V* curves; Table 2 lists the average values. The values of R_{sh} and R_s of the normal, M2005, M2070, D2000, and ED2003 devices were 1086 ± 314/2.0 ± 0.2, 1438 ± 628/1.9 ± 0.1, 975 ± 254/2.0 ± 0.1, 2118 ± 672/1.5 ± 0.2, and 1040 ± 632/2.0 ± 0.2 Ω cm^2, respectively. The values of R_s values (from 1.5 ± 0.2 to 2.0 ± 0.2 Ω cm^2) were similar for all of the devices, suggesting that their interfacial and bulk resistances were also similar. The previously reported values of R_s for PTB7-based inverted devices have been between 1.68 and 6.4 Ω cm^2.[46–48] The value of R_s described herein is among the lowest ever reported, reflecting the high FFs (>71%) of the devices. The slightly lower value of R_s for the D2000 device is consistent with it also having the best OPV performance. The value of R_{sh} typically correlates with the leakage current and the degree of unwanted free carrier recombination in a device.[7,28,49] The greater value of R_{sh} for the D2000 device might be due to its better interfacial status providing efficient and favorable electron selection and transport, thereby improving the device properties. Fig. 2b presents the IPCE responses for the devices. For the PTB7:PC$_{71}$BM devices, the response of the IPCEs occurred at wavelengths from 400 to 800 nm. The greatest IPCEs were those for the D2000-derived device, with a maximum of 76.4% at a wavelength of 620 nm. The values of J_{sc} of the ZnO, M2005, M2070, D2000, and ED2003 devices, calculated from the integration of the IPCE spectra with the AM 1.5G reference spectrum, were 14.2, 13.8, 13.8, 14.6, and 13.9 mA cm^{-2}, respectively; these values have mismatches of approximately 10% when compared with those obtained from a solar simulator (Table 2).

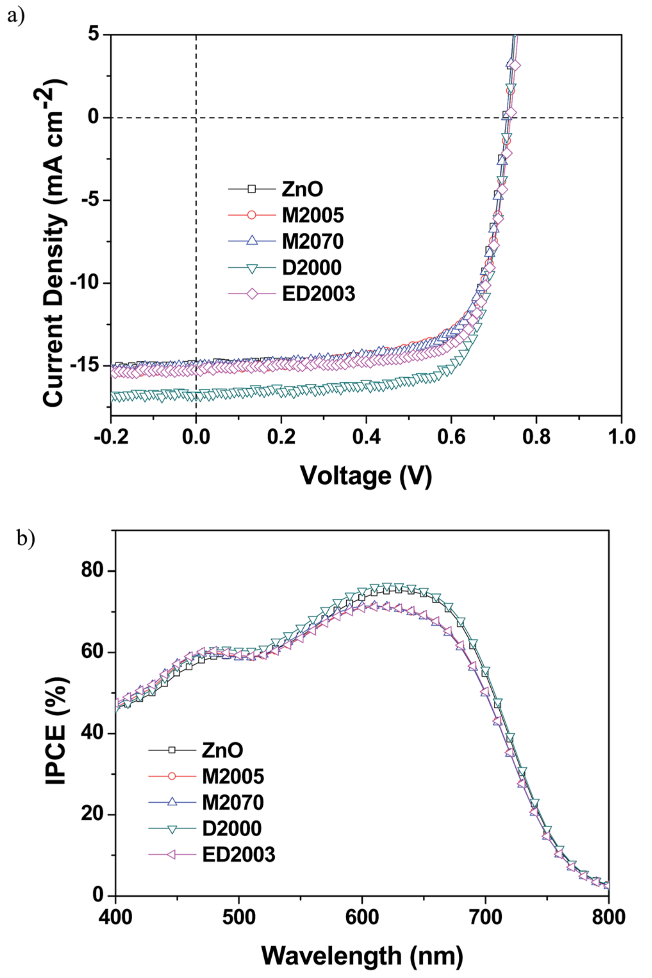

Fig. 2 (a) *I–V* characteristics and (b) IPCE responses of OPV devices prepared with various IFLs.

Fig. 3 and S2† present AFM images of the BHJ films deposited on various ZnO surfaces. The topographical images revealed that the root mean square (RMS) surface roughnesses of the ZnO-, M2005-, M2070-, D2000-, and ED2003-derived BHJ blend films were 1.25, 1.92, 1.36, 1.91, and 1.25 nm, respectively. These very small surface roughnesses suggested nanoscale phase segregated behavior. The AFM phase images of these blend films revealed that these active layers displayed well-defined nano-phase segregation, with a domain size of less than 50 nm and an interpenetration morphology (Fig. 3 and S2†); this structure is consistent with the excellent device performance, with average FFs of these devices being greater than 71% (Table 2). A closer look revealed differences in the phase images. The enlarged phase images (201 nm × 201 nm) in Fig. 3 feature two phase regions: dark regions representing fullerene-rich domains and bright domains representing PTB7-rich phases.[24] The blend film cast on the ZnO featured phase segregation of the PC$_{71}$BM-rich phase (domain size: <15 nm) surrounded by a PTB7-rich phase (10–25 nm). The D2000-derived blend film exhibited a larger phase separation domain in which the PC$_{71}$BM-rich domains having an irregular structure (domain sizes from several to tens of nanometers) were dispersed within a 25–40 nm PTB7-rich area. Because the D2000-derived blend film formed larger polymer domains, with larger PCBM domains dispersed well in the polymer matrix, and the D/A domain sizes of the D2000 film were within the efficient exciton diffusion length, this well-defined morphology facilitated the transmission of electrons and holes within the PTB7 and PCBM regions to the corresponding electrodes. In contrast, the possibility of unwanted carrier recombination was higher for the ZnO blend, due to its

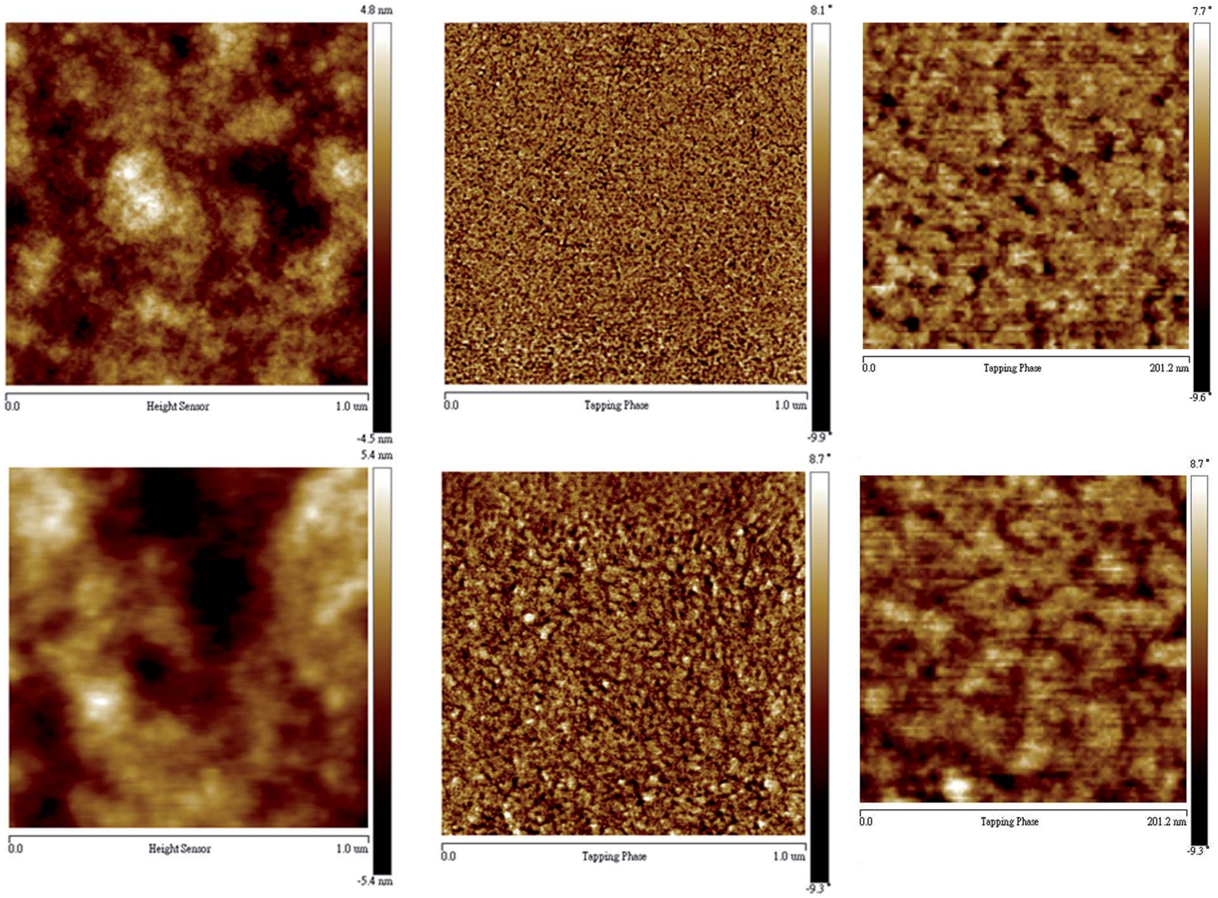

Fig. 3 AFM topographic (1 μm × 1 μm), phase (1 μm × 1 μm), and enlarge phase images (201 nm × 201 nm) of (a) ZnO- and (b) D2000-derived blend films.

smaller D/A domain size; hence, we observed lower values of R_{sh} and FF for the ZnO devices.

To understand why embedding D2000 significantly improved the FF and the value of J_{sc} value of the device, we employed SCLC electron mobility measurements and ultraviolet photoelectron spectroscopy (UPS) to observe whether or not this IFL changed the electron mobility or the WF; the electron mobility within the BHJ layer can be related to the electron extraction performance from the active layer/ETL interface.[16,50,51] We fabricated electron-only SCLC devices having the configuration ITO/ZnO (with or without D2000)/PTB7:PC$_{71}$BM/Ca/Al. The SCLC electron mobilities (averaged from five to seven devices) of the devices based on ZnO and D2000 were 1.24×10^{-8} ($\pm 1.86 \times 10^{-9}$) and 3.06×10^{-8} ($\pm 1.07 \times 10^{-9}$) m^2 V^{-1} s^{-1}, respectively. The devices prepared with interlayers of D2000 had a nearly 2.5-fold higher SCLC electron mobility, suggesting improved electron extraction from the PTB7/PCBM blend film. The factors that affected the carrier mobility (transportation in the BHJ and extraction at the interfaces) were presumably the differences in the morphologies of the active layers (observed through AFM) and the WFs. The incorporation of an IF layer having an amino functional group will typically build up an interfacial dipole that alters the WF of the electrode, thereby potentially facilitating efficient energy level pinning for high-performance carrier extraction.[15–17,34] To determine whether incorporating the Jeffamine played a role in changing the WF, we used UPS to compare the WFs of ITO/ZnO and ITO/ZnO/D2000. Fig. 4 presents the cutoff and valence band regions of the UPS spectra of the samples. After interlaying D2000, we observed a decrease in the WF of the ITO/ZnO substrate by 0.24 eV. By embedding an amine-based IF layer, the WF of ITO/ZnO would likely be reduced.[34] The change in the surface status would affect the energy level alignment at the interface between ITO/ZnO/D2000 and the active layer. The nitrogen and oxygen atoms in D2000 would function as donors that contact the surface of the ZnO film and change its WF by forming net dipoles (from the molecular and surface dipoles) at the interface (Fig. 4b).[24,51] The true WF of ITO/ZnO was −3.47 eV (consistent with the value reported in the literature); it decreased by 0.24 eV to −3.23 eV after embedding the D2000 interlayer.[52] The AFM data revealed that the phase segregation morphology of the BHJ changed after embedding the IF layers. Our results suggest that the surface status (surface energy, morphology and WF) of the substrate altered the local BHJ morphology and changed the degree of electron extraction in the cathode. Because this morphology prevented unfavorable charge recombination at the ETL interface, we observed improvement in the FF and performance. Determining the possible effects of embedding IF layers (from variations in electronics properties to variations in morphologies) can be challenging; our results provide an example that should allow better understanding of the role of the interfaces within OPV devices.

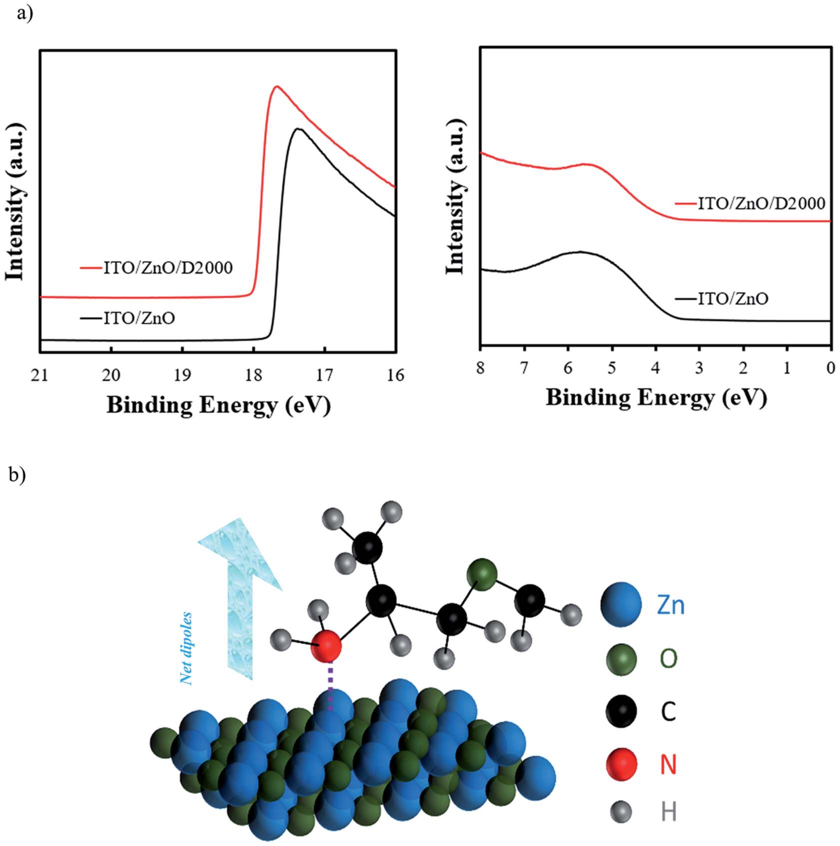

Fig. 4 (a) Photoemission cut-off and valence band regions, obtained using UPS, for ZnO with and without D2000; and (b) net dipole-induced change in the WF of the ZnO surface.

Conclusion

We have demonstrated that Jeffamines can be used as ETL modifying layers for high-performance OPVs. The incorporation of these materials changed the surface energy, thereby affecting the wetting properties of the active layer solution and, hence, altering the morphologies of the blend films. Compared with the performance of the normal device, the embedding of Jeffamine D2000 enhanced the charge extraction efficiency [from 1.24×10^{-8} ($\pm 1.86 \times 10^{-9}$) to 3.06×10^{-8} ($\pm 1.07 \times 10^{-9}$) $m^2\ V^{-1}\ s^{-1}$], due to a change in the WF of ZnO (with appropriate energy levels) and an improved blend film morphology for enhanced electron transportation and greater selectivity of the cathode. The PCE of the device embedding D2000 as the IF layer increased by 6.2% (from 8.1 ± 0.11 to 8.6 ± 0.37%) because of a significant increase in the FF. Because of the wide variety and low price of the Jeffamines, their judicious selection should result in the development of inexpensive cathode interlayers for large-area OPVs and other optoelectronic devices.

Experimental section

Materials and methods

All chemical reagents were obtained from Aldrich and used as received (unless noted otherwise). UV-Vis absorption spectroscopy was performed using a Hitachi U-5100 spectrophotometer. PTB7 was purchased from 1-Materials; the Jeffamines were obtained from Great Eastern Resins Industrial of Taichung, Taiwan.

Acknowledgements

We thank the Ministry of Science and Technology of Taiwan (MOST 103-2113-M-131-001-MY2; MOST 105-2221-E-131-033-) for financial support.

References

1 F. Pastorelli, T. M. Schmidt, M. Hösel, R. R. Søndergaard, M. Jørgensen and F. C. Krebs, *Adv. Eng. Mater.*, 2016, **18**, 51–55.
2 K. Liu, T. T. Larsen-Olsen, Y. Lin, M. Beliatis, E. Bundgaard, M. Jorgensen, F. C. Krebs and X. Zhan, *J. Mater. Chem. A*, 2016, **4**, 1044–1051.
3 C. J. M. Emmott, D. Moia, P. Sandwell, N. Ekins-Daukes, M. Hösel, L. Lukoschek, C. Amarasinghe, F. C. Krebs and J. Nelson, *Sol. Energy Mater. Sol. Cells*, 2016, **149**, 284–293.
4 Y. Yang, W. Chen, L. Dou, W.-H. Chang, H.-S. Duan, B. Bob, G. Li and Y. Yang, *Nat. Photonics*, 2015, **9**, 190–198.
5 L. Dou, Y. Liu, Z. Hong, G. Li and Y. Yang, *Chem. Rev.*, 2015, **115**, 12633–12665.
6 S. Dai, F. Zhao, Q. Zhang, T. K. Lau, T. Li, K. Liu, Q. Ling, C. Wang, X. Lu, W. You and X. Zhan, *J. Am. Chem. Soc.*, 2017, **139**, 1336–1343.

7 H. Kang, W. Lee, J. Oh, T. Kim, C. Lee and B. J. Kim, *Acc. Chem. Res.*, 2016, **49**, 2424–2434.

8 S. Zhang, L. Ye and J. Hou, *Adv. Energy Mater.*, 2016, **6**, 1502529.

9 J. Zhao, Y. Li, G. Yang, K. Jiang, H. Lin, H. Ade, W. Ma and H. Yan, *Nat. Energy*, 2016, **1**, 15027.

10 G. Luo, X. Ren, S. Zhang, H. Wu, W. C. H. Choy, Z. He and Y. Cao, *Small*, 2016, **12**, 1547–1571.

11 X. Ren, J. Cheng, S. Zhang, X. Li, T. Rao, L. Huo, J. Hou and W. C. H. Choy, *Small*, 2016, **12**, 5102.

12 X. Ren, J. Cheng, S. Zhang, X. Li, T. Rao, L. Huo, J. Hou and W. C. H. Choy, *Small*, 2016, **12**, 5200–5207.

13 B. Yang, S. Zhang, Y. Chen, Y. Cui, D. Liu, H. Yao, J. Zhang, Z. Wei and J. Hou, *Macromolecules*, 2017, **50**, 1453–1462.

14 Q. Fan, W. Su, X. Guo, X. Zhang, Z. Xu, B. Guo, L. Jiang, M. Zhang and Y. Li, *J. Mater. Chem. A*, 2017, **5**, 5106–5114.

15 Z. Yin, J. Wei and Q. Zheng, *Adv. Sci.*, 2016, **3**, 1500362.

16 C.-C. Chueh, C.-Z. Li and A. K. Y. Jen, *Energy Environ. Sci.*, 2015, **8**, 1160–1189.

17 B. Xiao, H. Wu and Y. Cao, *Mater. Today*, 2015, **18**, 385–394.

18 C. Yi, X. Hu, X. Gong and A. Elzatahry, *Mater. Today*, 2016, **19**, 169–177.

19 Z. George, Y. Xia, A. Sharma, C. Lindqvist, G. Andersson, O. Inganas, E. Moons, C. Muller and M. R. Andersson, *J. Mater. Chem. A*, 2016, **4**, 2663–2669.

20 T. P. Le, Z. Shang, L. Wang, N. Li, S. Vajjala Kesava, J. W. O'Connor, Y. Chang, C. Bae, C. Zhu, A. Hexemer, E. W. Gomez, A. Salleo, M. A. Hickner and E. D. Gomez, *Macromolecules*, 2015, **48**, 5162–5171.

21 Y. Cui, B. Xu, B. Yang, H. Yao, S. Li and J. Hou, *Macromolecules*, 2016, **49**, 8126–8133.

22 J. Kesters, S. Govaerts, G. Pirotte, J. Drijkoningen, M. Chevrier, N. Van den Brande, X. Liu, M. Fahlman, B. Van Mele, L. Lutsen, D. Vanderzande, J. Manca, S. Clément, E. Von Hauff and W. Maes, *ACS Appl. Mater. Interfaces*, 2016, **8**, 6309–6314.

23 S. Nam, J. Seo, S. Woo, W. H. Kim, H. Kim, D. D. Bradley and Y. Kim, *Nat. Commun.*, 2015, **6**, 8929.

24 T.-Y. Juang, Y.-C. Hsu, B.-H. Jiang and C.-P. Chen, *Macromolecules*, 2016, **49**, 7837–7843.

25 H.-L. Hsu, T.-Y. Juang, C.-P. Chen, C.-M. Hsieh, C.-C. Yang, C.-L. Huang and R.-J. Jeng, *Sol. Energy Mater. Sol. Cells*, 2015, **140**, 224–231.

26 N. Chakravarthi, K. Gunasekar, W. Cho, D. X. Long, Y.-H. Kim, C. E. Song, J.-C. Lee, A. Facchetti, M. Song, Y.-Y. Noh and S.-H. Jin, *Energy Environ. Sci.*, 2016, **9**, 2595–2602.

27 J. Cheng, X. Ren, H. L. Zhu, J. Mao, C. Liang, J. Zhuang, V. A. L. Roy and W. C. H. Choy, *Nano Energy*, 2017, **34**, 76–85.

28 M.-H. Jao, H.-C. Liao and W.-F. Su, *J. Mater. Chem. A*, 2016, **4**, 5784–5801.

29 J. Han, Y. Chen, W. Chen, C. Yu, X. Song, F. Li and Y. Wang, *ACS Appl. Mater. Interfaces*, 2016, **8**, 32823–32832.

30 W. Yu, L. Huang, D. Yang, P. Fu, L. Zhou, J. Zhang and C. Li, *J. Mater. Chem. A*, 2015, **3**, 10660–10665.

31 L. Zhou, W. Yu, S. Yu, P. Fu, X. Guo and C. Li, *J. Mater. Chem. A*, 2017, **5**, 657–662.

32 S. Woo, W. Hyun Kim, H. Kim, Y. Yi, H.-K. Lyu and Y. Kim, *Adv. Energy Mater.*, 2014, **4**, 1301692.

33 B. Cao, X. He, C. R. Fetterly, B. C. Olsen, E. J. Luber and J. M. Buriak, *ACS Appl. Mater. Interfaces*, 2016, **8**, 18238–18248.

34 Y. Zhou, C. Fuentes-Hernandez, J. Shim, J. Meyer, A. J. Giordano, H. Li, P. Winget, T. Papadopoulos, H. Cheun, J. Kim, M. Fenoll, A. Dindar, W. Haske, E. Najafabadi, T. M. Khan, H. Sojoudi, S. Barlow, S. Graham, J.-L. Brédas, S. R. Marder, A. Kahn and B. Kippelen, *Science*, 2012, **336**, 327–332.

35 P. Li, G. Wang, L. Cai, B. Ding, D. Zhou, Y. Hu, Y. Zhang, J. Xiang, K. Wan, L. Chen, K. Alameh and Q. Song, *Phys. Chem. Chem. Phys.*, 2014, **16**, 23792–23799.

36 C. C. Huang, C. H. Lin and S. A. Dai, *J. Polym. Sci., Part A: Polym. Chem.*, 2016, **54**, 802–808.

37 J. Yan, Q. Liang, K. Liu, J. Miao, H. Chen, S. Liu, Z. He, H. Wu, J. Wang and Y. Cao, *ACS Energy Lett.*, 2017, **2**, 14–21.

38 J.-L. Wang, K.-K. Liu, J. Yan, Z. Wu, F. Liu, F. Xiao, Z.-F. Chang, H.-B. Wu, Y. Cao and T. P. Russell, *J. Am. Chem. Soc.*, 2016, **138**, 7687–7697.

39 Y. Wei, P.-J. Liu, R.-H. Lee and C.-P. Chen, *RSC Adv.*, 2015, **5**, 7897–7904.

40 X. Bulliard, S.-G. Ihn, S. Yun, Y. Kim, D. Choi, J.-Y. Choi, M. Kim, M. Sim, J.-H. Park, W. Choi and K. Cho, *Adv. Funct. Mater.*, 2010, **20**, 4381–4387.

41 K.-J. Chang, F.-Y. Yang, C.-C. Liu, M.-Y. Hsu, T.-C. Liao and H.-C. Cheng, *Org. Electron.*, 2009, **10**, 815–821.

42 Y.-A. Su, W.-C. Lin, H.-J. Wang, W.-H. Lee, R.-H. Lee, S. A. Dai, C.-F. Hsieh and R.-J. Jeng, *RSC Adv.*, 2015, **5**, 25192–25203.

43 C.-P. Chen and H.-L. Hsu, *Macromol. Rapid Commun.*, 2013, **34**, 1623–1628.

44 W. Chen, J. Lv, J. Han, Y. Chen, T. Jia, F. Li and Y. Wang, *J. Mater. Chem. A*, 2016, **4**, 2169–2177.

45 X. Jin, Y. He, C. Liu, F. Wu, Y. Xu, L. Huang, L. Chen and Y. Chen, *Sol. Energy Mater. Sol. Cells*, 2016, **157**, 644–651.

46 Z. Lin, J. Chang, C. Zhang, J. Zhang, J. Wu and Y. Hao, *J. Mater. Chem. C*, 2016, **4**, 6169–6175.

47 H. Yang, T. Wu, T. Hu, X. Hu, L. Chen and Y. Chen, *J. Mater. Chem. C*, 2016, **4**, 8738–8744.

48 X. Lin, Y. Yang, L. Nian, H. Su, J. Ou, Z. Yuan, F. Xie, W. Hong, D. Yu, M. Zhang, Y. Ma and X. Chen, *Nano Energy*, 2016, **26**, 216–223.

49 K. Wang, C. Liu, T. Meng, C. Yi and X. Gong, *Chem. Soc. Rev.*, 2016, **45**, 2937–2975.

50 E. J. Lee, S. W. Heo, Y. W. Han and D. K. Moon, *J. Mater. Chem. C*, 2016, **4**, 2463–2469.

51 B. A. E. Courtright and S. A. Jenekhe, *ACS Appl. Mater. Interfaces*, 2015, **7**, 26167–26175.

52 H. H. Kim, S. Park, Y. Yi, D. I. Son, C. Park, D. K. Hwang and W. K. Choi, *Sci. Rep.*, 2015, **5**, 8968.